ARTICLE
Journal of Cellular Biochemistry 114:658–668 (2013)

Journal of Cellular Biochemistry

Suppression of Mammalian Bone Growth by Membrane Transport Inhibitors

Mohamad Y. Loqman,[1] Peter G. Bush,[2] Colin Farquharson,[3] and Andrew C. Hall[1*]

[1] *Centre for Integrative Physiology, School of Biomedical Sciences, George Square, University of Edinburgh, Edinburgh EH8 9XD, Scotland, UK*

[2] *School of Pharmacy and Biomolecular Sciences, University of Brighton, Lewes Road, Brighton BN2 4GJ, England, UK*

[3] *Division of Developmental Biology, The Roslin Institute, R(D)SVS, University of Edinburgh, Easter Bush EH25 9RG, Scotland, UK*

ABSTRACT

Bone lengthening during skeletal growth is driven primarily by the controlled enlargement of growth plate (GP) chondrocytes. The cellular mechanisms are unclear but membrane transporters are probably involved. We investigated the role of the Na^+/H^+ antiporter (NHE1) and anion exchanger (AE2) in bone lengthening and GP chondrocyte hypertrophy in Sprague–Dawley 7-day-old rat (P7) bone rudiments using the inhibitors EIPA (5-(*N*-ethyl-*N*-isopropyl)amiloride) and DIDS (4,4-diidothiocyano-2,2-stilbenedisulphonate), respectively. We have also determined cell-associated levels of these transporters along the GP using fluorescent immunohistochemistry (FIHC). Culture of bones with EIPA or DIDS inhibited rudiment growth (50% at approx. 250 and 25 μM, respectively). Both decreased the size of the hypertrophic zone ($P < 0.05$) but had no effect on overall length or cell density of the GP. In situ chondrocyte volume in proliferative and hypertrophic zones was decreased ($P < 0.01$) with EIPA but not DIDS. FIHC labeling of NHE1 was relatively high and constant along the GP but declined steeply in the late hypertrophic zone. In contrast, AE2 labeling was relatively low in proliferative zone cells but increased ($P < 0.05$) reaching a maximum in the early hypertrophic zone, before falling rapidly in the late hypertrophic zone suggesting AE2 might regulate the transition phase of chondrocytes between proliferative and hypertrophic zones. The inhibition of bone growth by EIPA may be due to a reduction to chondrocyte volume set-point. However the effect of DIDS was unclear but could result from inhibition of AE2 and blocking of the transition phase. These results demonstrate that NHE1 and AE2 are important regulators of bone growth. J. Cell. Biochem. 114: 658–668, 2013.

KEY WORDS: GROWTH PLATE; CHONDROCYTE; HYPERTROPHY; EIPA; DIDS

The growth plate comprises a relatively thin layer of cells (chondrocytes) arranged in columns which lie perpendicular to, and are entirely responsible for, new bone formation during longitudinal growth of the skeleton. The chondrocytes are highly organized with a ''reserve zone'' preceding the proliferative zone chondrocytes (PZC) which are relatively small and flattened. However after a specific time period, differentiation of the chondrocytes occurs leading to a dramatic increase in volume and the formation of hypertrophic zone chondrocytes (HZC). The cell volume, which for example in 7-day-old (P7) rat proximal tibia can increase dramatically from approximately 1,000–10,000 μm^3 [Bush et al., 2008b], is mainly in the longitudinal axis, and accounts for 60–80% of bone lengthening [Wilsman et al., 1996ab, 2008]. There is a positive linear relationship between the rate of longitudinal bone growth over 24 h and the final volume of hypertrophic chondrocytes [Breur et al., 1991].

The increase in cell volume occurs by both cell swelling [increasing water content of cells; Buckwalter et al., 1996] and also classical hypertrophy [increase in cell mass; Bush et al., 2008b] however the mechanism which drives the enlargement of GP

Grant sponsor: Biotechnology and Biological Sciences Research Council; Grant numbers: BB/C513985/1, Strategic Programme Grant.

Mohamad Y. Loqman's present address is Faculty of Veterinary Medicine, Department of Veterinary Clinical Studies, Universiti Putra Malaysia, Serdang, Selangor 43400, Malaysia.

*Correspondence to: Andrew C. Hall, Centre for Integrative Physiology, School of Biomedical Sciences, George Square, University of Edinburgh, Edinburgh EH8 9XD, Scotland, UK. E-mail: a.hall@ed.ac.uk

Manuscript Received: 9 July 2012; Manuscript Accepted: 21 September 2012

Accepted manuscript online in Wiley Online Library (wileyonlinelibrary.com): 11 October 2012

DOI 10.1002/jcb.24408 • © 2012 Wiley Periodicals, Inc.

chondrocytes is poorly understood. The controlled increase in chondrocyte size and the regulation of the intracellular environment (e.g., ion content, pH_i) to permit optimal metabolism must be closely regulated throughout the hypertrophic process mainly by the activity of the membrane transporters in the chondrocyte membrane. It is likely that there is an important role for transporters which regulate the movement of Na^+ and anions (e.g., HCO_3^-) across the cell membrane as these are known to be essential for the control of cell volume and pH_i in a wide range of cell types [Hoffmann et al., 2009].

Our previous studies have shown a role for the NKCC cotransporter (NKCC1) in mediating growth plate chondrocyte hypertrophy [Bush et al., 2010]. Incubating growing metatarsals/metacarpals from P7 rat pups in the presence/absence of the specific inhibitor bumetanide demonstrated a 35% inhibition of bone growth suggesting that other, as yet unidentified, membrane transporters could also promote chondrocyte hypertrophy and thus bone growth. The two other transporters that could potentially be involved because of their contribution to cell volume and pH_i regulation, are the Na^+/H^+ exchanger (NHE) and the anion exchanger (AE) and it is the purpose of this study to clarify their possible role in bone growth.

Since the discovery of the Na^+/H^+ exchanger, nine NHE isoforms have been identified. NHE1 was the first identified and is distinct in that it is ubiquitously expressed in all mammalian cells and plays a "housekeeping" role in the regulation of pH_i and cell volume [Malo and Fliegel, 2006]. This isoform was the most sensitive to amiloride and its derivatives [e.g., EIPA; 5-(*N*-ethyl-*N*-isopropyl)amiloride; Masereel et al., 2003]. NHE1 is the key regulator of pH_i in the majority of articular chondrocytes within hyaline cartilage [Tattersall and Wilkins, 2008] however cells within the superficial zone utilize a HCO_3^--dependent process [Simpkin et al., 2007]. Increased activity of NHE1 combined with the parallel activation of the anion exchanger isoform AE2 occurs following the shrinking of cells in media of raised osmolarity. This gives rise to the recovery of cell volume through the process of regulatory volume increase (RVI) and also the maintenance of pH_i in the face of the osmotic challenge [Shen et al., 2002; Liu et al., 2011]. Activation of these transporters *without* a change in extracellular osmotic pressure, will directly increase cell volume and re-set pH_i [Hoffmann et al., 2009] and therefore could be a mechanism utilized by GP chondrocytes to drive cell enlargement and maintain pH_i during hypertrophy.

This study therefore extends previous work by testing the hypothesis that NHE1 and AE2 are involved in the regulation of longitudinal growth in mammalian long bones. We incubated metatarsal rudiments from P7 rats in the presence of EIPA or DIDS (4,4-diidothiocyano-2,2-stilbenedisulphonate; a relatively non-specific inhibitor of AE2), and observed almost complete inhibition of bone growth. The height of the hypertrophic zone (HZ) of the growth plate in the presence of these drugs was significantly reduced, but there was no change in cell density or viability. We found that with DIDS there was no significant change to the volume of in situ PZ or HZ chondrocytes, however with EIPA treatment, there was a significant reduction cell size. Using fluorescent immunohistochemistry (FIHC), we observed relatively high levels of cell-associated NHE1 labeling which declined in the latter stages of hypertrophy. In contrast, AE2 labeling was initially low, but increased significantly until early hypertrophy, and then decreased significantly at the final stages of chondrocyte hypertrophy. These results suggest that both transporters are essential for bone growth.

MATERIALS AND METHODS

BIOCHEMICALS AND SOLUTIONS

Biochemicals were obtained from Invitrogen Ltd. (Paisley, UK) unless otherwise indicated. The following culture media were used: (a) *Dissection media* which comprised PBS with 7.5% (v/v) α-modified essential medium (α-MEM) and 2% (w/v) bovine serum albumin V (300mOsm; pH 7.4). (b) *Standard culture media* which contained α-MEM supplemented with: Na_2 glycerol bi-phosphate (1 mM); bovine serum albumin (BSA, Fraction V, 0.2% (w/v) 5 mg/ml; L-ascorbic acid 1% (v/v); penicillin and streptomycin (final concentrations of 100 IU/ml and 100 μg/ml, respectively; 300mOsm; pH 7.4). The anion exchange (AE) inhibitor DIDS (4,4-diidothiocyano-2,2-stilbenedisulphonate) was prepared fresh for each experiment as a 100 mM stock solution in 0.1 M $KHCO_3$. The Na^+/H^+ exchange inhibitor EIPA (5-(*N*-ethyl-*N*-isopropyl)-amiloride) was prepared as a 120 mM stock solution in DMSO. The antibodies used were rabbit polyclonals to NHE1 (ab67313, Abcam, Cambridge, UK) and AE2 (ab42687, Abcam). The fluorescent dyes CMFDA (5-chloromethylfluorescein diacetate) and propidium iodide (PI) were dissolved in a small amount of DMSO, and made up with PBS to a 10 mM stock.

ANIMALS, BONES, AND GROWTH PLATE PREPARATION

Sprague–Dawley rat pups (P7) were humanely killed for other experiments following Home Office guidelines. Rudiments from the middle three metatarsals with intact growth plates were carefully removed and temporarily placed in dissection medium. For the ex vivo cultures, the overall length of the rudiments were measured using an eyepiece camera (DCM35 Pixel Digital Eyepiece Camera, Brunel Microscopes, Chippenham, Wiltshire, UK) fitted to a stereomicroscope (Leica Geosystems, Heerbrugg, Switzerland). An image of a rule was acquired to provide calibration, and bone lengths measured (to 0.1 mm) using ImageJ software (NIH, Bethesda, MD). Results were expressed as a percentage change from the length at day 0. Rudiments were placed individually in each well of a 24-well plate and then incubated in 1 ml of standard culture medium (5% CO_2, 95% air, pH 7.4, 37°C) supplemented with the drugs as described in Results Section. These bones were chosen since at P7 bone mineralization was at a minimum and the preparation of histological sections could be performed by avoiding the possibly immuno-compromising bone decalcification step.

PREPARATION OF GROWTH PLATES FOR HISTOLOGY

Bones were fixed overnight in 1.3% glutaraldehyde (GA) with 0.5% ruthenium hexamine trichloride (RHT; pH 7.4) with osmolarity adjusted to 300 mOsm to avoid fixative-induced artefacts to chondrocyte shape/volume [Loqman et al., 2010]. Bones were then dehydrated through a series of ethanol solutions and embedded in paraffin wax using a standard procedure [Kiernan, 1999]. Bones were then cut into longitudinal 10 μm serial sections (Reichert–Jung Microtome 2050 Supercut, Arnsberg, Germany).

After de-paraffinization with xylene and rehydration with a series of ethanol solutions (100%, 90%, and 75%), the sections were stained with 0.1% toluidine blue O in PBS (pH 5.5; 30 s at 21°C) using the technique adapted from Bancroft and Cook [1994]. The sections were then mounted on poly-L-lysine-coated microscope slides (Polysine™, VWR International, Leicestershire, UK) rinsed briefly in distilled water, and air dried prior to mounting with Fluorosave™ and coverslips.

MEASUREMENT OF GROWTH PLATE LENGTH AND CELL DENSITY

Images of distal growth plates were taken using the transmitted light detector of an upright confocal laser scanning microscope (Zeiss LSM510) fitted with a 10× (N.A. [numerical aperture] = 0.3) dry objective lens. To determine the beginning and terminal points of the GP, several subjective criteria based on cell size and organization were used as described [Hunziker, 1994]. The GP length and the late HZ height were then identified and measured using an established procedure [see Bush et al., 2010]. Briefly, three zones were identified by eye and marked by drawing a freehand line (i) along the top of the proliferating cell border, (ii) along the clear demarcation of cell enlargement between proliferative and hypertrophic regions, and (iii) the zone of mineralization at the base of the hypertrophic zone. Using these lines of demarcation and the orientation of the cell columns as a guide, a vertical line was drawn through the mid-GP sections (Zeiss LSM Image Browser Software, Carl Zeiss MicroImaging GmbH, Germany; Fig. 2). The GP length between the two points where the vertical and horizontal lines met most proximally and distally, was measured using ImageJ software (NIH). The late HZ height was determined from the distance between the two points where the lines met at the PZ–HZ cell enlargement regions proximally and the zone of mineralization distally. The total number of cells within the late hypertrophic zone was counted by eye, and the surface area of the zone was selected using freehand selection and measured using ImageJ. The cell density was determined based on the total cell numbers counted over the measured area of the late HZ (cells/mm^2).

FLUORESCENT LABELING OF IN SITU GROWTH PLATE CHONDROCYTES

For the analysis of GPC viability, bones were incubated in standard culture medium supplemented with inhibitors at the following concentrations; (i) 0 μM DIDS ($KHCO_3$ vehicle alone), (ii) 250 μM DIDS, (iii) 0 μM EIPA (DMSO vehicle alone), and (iv) 444 μM EIPA. Bone rudiments were maintained at 37°C for 24 h as described above. Bones were then washed in fresh culture media before being bisected sagitally with a fresh scalpel blade for each cut [Amin et al., 2008], and incubated with CMFDA, and PI (both at 5 μM; 60 min; 37°C). CMFDA is permeable only to viable cells, and in the cytoplasm is metabolized by cellular esterases to produce a membrane-impermeant fluorescent product that stains the cytoplasm of viable cells green. PI however is only capable of crossing plasma membranes of dying/dead cells and stains the nuclei of the dead cells, red [Amin et al., 2008]. Bones were then fixed in 4% (v/v) paraformaldehyde overnight, and stored at 4°C in PBS until visualized by confocal scanning laser microscopy (CLSM). The analysis of chondrocyte volume was performed using 3D imaging software (Volocity®, Improvision, Coventry, UK) on scanned confocal scanning laser microscopy (CLSM) images using the calibrated cell volume method as previously described [Loqman et al., 2010]. Chondrocyte viability was evaluated by estimating the proportion of PI-labeled chondrocytes compared to the total labeled cell population (CMFDA + PI-labeled) within comparable regions of interest (ROIs) in the growth plates of bones cultured under the different conditions. For experiments on living/unfixed in situ chondrocytes, GPs were incubated with calcein-AM and PI (30 min; 5 μM each; 37°C) and imaged as described [Loqman et al., 2010].

FLUORESCENT IMMUNOHISTOCHEMISTRY (FIHC)

On each slide, typically 3–4 sections were designated as negative controls while the other 2–3 underwent normal Ab labeling. Non-specific Ab sites were blocked using goat serum (1:5 dilution; 30 min; 21°C) and then replaced by the specific 1° antibodies (Abs) under investigation. Optimal dilution of the 1° Ab was determined using a series of different titres [Renshaw, 2007] and for the negative control sections, the 1° Ab was omitted. Slides were then incubated overnight at 4°C in a humidity chamber, then washed 3× (5 min each) with PBS before being incubated with a FITC (fluorescein isothiocyanate)-tagged 2° Ab at 37°C for 1 hr. Sections were then washed 3× (5 min each) with PBS. Next, coverslips were mounted using Fluorosave™, slides wrapped in aluminium foil and left to dry (3 h; 4°C) prior to imaging by CLSM.

MEASUREMENT OF NHE1 AND AE2 CELL-ASSOCIATED FLUORESCENT LABELING

In order to measure cell-specific immunofluorescence staining intensity of individual chondrocytes, cells along the length of the GP were visualized at high magnification (63×, N.A. = 0.95; oil immersion objective) by CLSM. GP images in sequential zones were then "stitched" together to produce a montage of the whole length of a GP from the proliferative to hypertrophic zone. Each imaged growth plate was divided into eight equal sections (S1–S8) as described [Loqman et al., 2010]. The average fluorescence labeling intensity associated with AE2 or NHE1 Abs in individual cells was determined along the GP in an unbiased semi-quantitative manner using ImageJ Java-based scientific image processing software as described [Bush et al., 2010].

CONFOCAL LASER SCANNING MICROSCOPY (CLSM)

An upright Zeiss Axioskop LSM 510 (Carl Zeiss Ltd., Welwyn Garden City, Herts, UK) was used to acquire fluorescent images of in situ GPC. Cells were visualized using a Plan-Neofluar 10× dry objective (N.A. = 0.3) for low power overviews and 63× lens for high magnification views. Fluorescent-labeling of intact cells was performed by visualizing intracellular calcein or CMFDA excited using an Argon laser (488 nm) and emitted fluorescence detected at 517 nm using a 500–550 nm band pass filter. PI (propidium iodide) bound to nucleic acids of dead cells was excited using a He–Ne laser (543 nm) and emitted fluorescence detected using a 560 nm long pass filter. The pinhole was set at 1.00 Airy unit, and optimal imaging quality determined by varying laser power and detector sensitivity. The scanning speed was typically 0.6 Hz with two frame

integration of a 512×512 pixel image, with serial 1 μm z-step optical sections [see Bush and Hall, 2001ab; Bush et al., 2007 for details].

PRESENTATION OF RESULTS AND STATISTICAL ANALYSIS OF DATA

Data were expressed as means ± SEM from a minimum of three bones from (n) separate animals and (N) chondrocytes at each condition with data shown as (n[N]). Statistical significance between two groups was evaluated using two-tailed unpaired Student's *t*-tests, with trends in data sets analyzed using a one-way ANOVA. Statistical tests were performed using SigmaPlot® (ver. 11.0; Systat Software Inc., GmbH, Erkrath, Germany) and *P*-values considered significant when $P < 0.05$.

RESULTS

DOSE–RESPONSE INHIBITION OF BONE GROWTH BY DIDS OR EIPA

In order to study the roles of AE and NHE on bone lengthening, dose–response experiments were performed (Fig. 1A,B). The mean increase in bone length from the initial value in the DIDS control medium was 6.2 ± 1.3% (n = 4) over 24 h (Fig. 1A). Exposure to increasing DIDS concentrations up to 1 mM resulted in dose-dependent reduction of bone lengthening. This was most dramatic at 50 μM DIDS, with bone lengthening significantly reduced to 1.9 ± 0.9% (n = 4; $P < 0.05$). All DIDS concentrations resulted in a significant reduction in longitudinal growth ($P < 0.05$; n = 4). A DIDS concentration of 250 μM appeared to give maximal inhibition and was therefore used for subsequent studies. Figure 1B illustrates the effect of EIPA (0–1.3 mM) on metatarsal bone longitudinal growth. The mean increase in length after 24 h for control bones was 7.9 ± 0.5% (n = 36) and although the drug vehicle was different ($KHCO_3$ vs DMSO for DIDS and EIPA, respectively) the difference was not significant ($P > 0.05$). EIPA resulted in a dose-dependent decrease in bone lengthening, but only became significantly reduced at an EIPA concentration at 111 μM and above ($P < 0.05$). Whilst an EIPA concentration of 1.3 mM showed maximum reduction of bone lengthening (1.4 ± 0.3%), 444 μM was considered to be the concentration that produced the optimal reduction of bone lengthening and was therefore used in the later experiments. The concentrations of DIDS or EIPA resulting in a 50% inhibition were approximately 25 and 250 μM, respectively. For both drugs, there was a significant decrease in overall bone longitudinal growth inhibition as the DIDS or EIPA concentrations were increased (one-way ANOVA; $P < 0.001$).

There might be concern that these drugs could induce relatively non-specific cell death leading to an apparent inhibition of bone lengthening. Accordingly a cell viability test was performed on the GPC of metatarsal bones after 24 h of treatment with 250 μM DIDS or 444 μM EIPA with appropriate controls. Bones were then bisected and incubated with CMFDA and PI and the cells visualized by CLSM. There was no difference in the proportion of live:dead chondrocytes in any of the samples (data not shown) suggesting that these drugs were not inhibiting bone lengthening by causing the death of GPC.

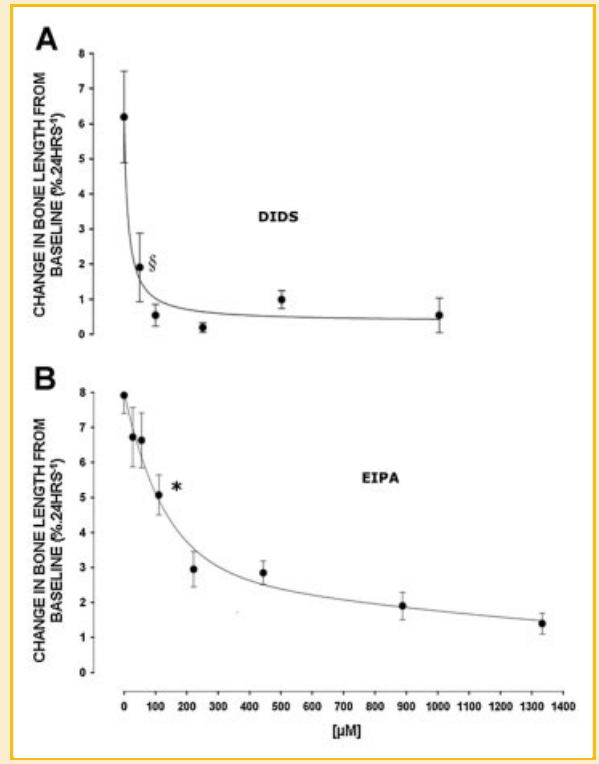

Fig. 1. The inhibitory effect of (A) DIDS and (B) EIPA on rat metatarsal bone rudiment growth. DIDS or EIPA were prepared with the appropriate vehicles at the concentrations shown (A and B, respectively), and the mean increase in bone length following culture for 24 h determined as described (see Materials and Methods Section). For both drugs, there was a significant inhibition in bone growth with increasing concentration (one-way ANOVA; $P < 0.001$). As shown, for a DIDS concentration of 50 μM, there was a significant decrease in bone lengthening compared to the control (no DIDS–vehicle only; $^{\S}P < 0.05$; unpaired Student's *t*-test) and this was the case for all higher DIDS concentrations ($P < 0.01$). For EIPA at 100 μM there was a significant inhibition compared to the control ($P < 0.05$), and this was also the case for all higher EIPA concentrations ($P < 0.01$). Data shown for each drug are means ± SEM for a minimum of four metatarsals from four different animals at each drug concentration.

CHANGES TO GP LENGTH, LATE HZ HEIGHT, AND CELL DENSITY FOLLOWING TREATMENT WITH DIDS OR EIPA

Having recorded the dose–response inhibition by DIDS or EIPA on ex vivo bone longitudinal growth (Fig. 1), the histological changes were examined. Emphasis was placed on the GP HZ cells, as the size of these cells is a determinant of the rate of longitudinal bone growth [Wilsman et al., 1996b] The total length of the GP, the height of the late HZ and the cell density in the late HZ were measured (Fig. 2). Table I shows the results of the metatarsals cultured in the presence or absence of DIDS (250 μM) or EIPA (444 μM). There was no significant difference in the total GP length between the control and DIDS-treated group (unpaired Student's *t*-test; $P > 0.05$; n = 4–6). Similarly there was no significant difference between the control and EIPA-treated group ($P > 0.05$). The height of the HZ in the DIDS-treated GP was also not significantly different from the untreated bones ($P > 0.05$). Likewise, there was no significant difference between the height of the HZ in the control compared to

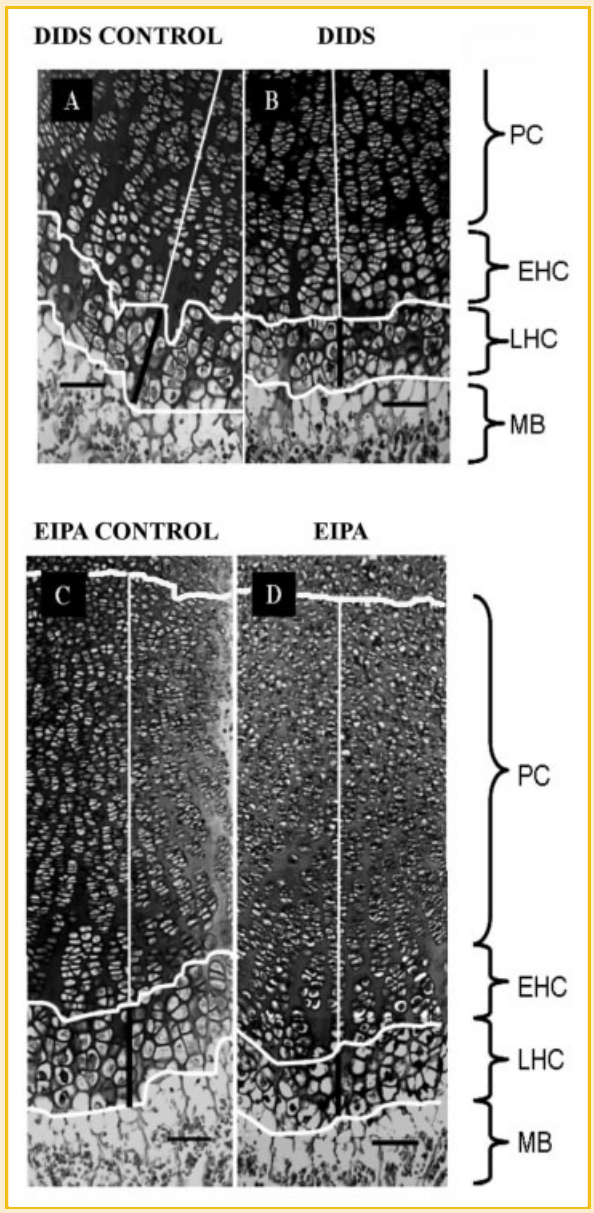

Fig. 2. The height of the late hypertrophic GP zone decreased significantly in the presence of DIDS or EIPA. Following 24 h culture with 250 μM DIDS or 444 μM EIPA, P7 rat metatarsal bones were fixed, and sections prepared and stained with 0.1% Toluidine blue O. Using light microscopy, the proximal GP was located and the late GP hypertrophic zone cells (LHC) identified by eye in between the beginning of the late hypertrophic zone cells and the mineralized bone (MB) at the bottom (between the two horizontal lines). The vertical black line at the mid GP section and between the two horizontal lines indicated the average height of the late hypertrophic GP zone in DIDS and EIPA-treated bones (B and D), and the controls (A and C). The straight black and white vertical lines at the mid GP section were used to determine the total length of the GP (see Materials and Methods Section). PC, proliferating zone cells (note that the bracket identifying these cells in A and B has been left open and the rest of the cells not included, because of the length of the zone); EHC, early hypertrophic zone cells. Scale bar = 100 μm in all panels.

the DIDS-treated GP ($P > 0.05$). Due to potential variation in the alignment of the metatarsals in the microtome and its cutting angle, the variability in measurements can be quite large making it less likely that significant differences could be recorded. However, when the data were normalized as described (see Materials and Methods Section) and the relative height of the HZ expressed as a percentage of the total GP length, the DIDS and EIPA-treated groups were significantly less compared to their controls ($P < 0.05$; $n = 4–6$). This suggests that in the presence of DIDS or EIPA, the reduction in the heights of the HZ over the length of the GP could account for the perturbation of normal GPC hypertrophy and thus the inhibition of bone lengthening by these drugs.

The reduction in the size of the late HZ height over the total GP length could be due to a decrease in cell density (e.g., caused by cell death), and/or changes in GPC size (e.g., caused by perturbation of normal cell enlargement). To further investigate this, the cell density in the HZ was measured. The results (Table I) showed no difference of GPC in the HZ of the DIDS or EIPA-treated metatarsals compared to the controls ($P > 0.05$) suggesting that these drugs did not cause significant loss/death of hypertrophic GPC.

EFFECT OF DIDS OR EIPA ON THE VOLUME OF IN SITU GPC

A more likely action of these drugs on bone lengthening could be by inhibiting the increase in cell volume during the transition from the proliferative to hypertrophic phenotype. The effects of DIDS or EIPA on in situ GPC volume were therefore determined using fluorescently labeled in situ chondrocytes and CLSM. Volume analysis was performed at the PZ (S1–S2) and the HZ (S7–S8; see Materials and Methods Section). Using a high power objective lens, no significant difference was observed in the volume of HZ GPC treated with DIDS and the control (Fig. 3A,B). However there was a clear reduction in HZC size between the EIPA-treated GPC and the control (Fig. 3C,D). Quantitative analysis of cell volume was also performed on the GPC in the PZ and HZ from the metatarsal bones of each treatment group (Table II). The results showed the mean volume of the control cells in PZ was not significantly different from DIDS-treated cells ($P > 0.05$). Likewise, the mean volume of the control cells in the HZ was not significantly different from the mean GPC volume in DIDS-treated cells ($P > 0.05$). On the other hand, there was a significant decrease in the volume of the EIPA-treated cells in the PZ and the HZ compared to the control cells (unpaired Student's t-test; $P < 0.05$; $n = 3–6$; Table II). Taken together, these data show that DIDS treatment resulted in no significant changes to the size of the PZ cells and HZ cells whereas EIPA treatment resulted in a significant reduction in size of these cells.

FLUORESCENT IMMUNOHISTOCHEMISTRY OF NHE1 AND AE2 IN P7 RAT GPC

Low power CLSM images showed no detectable NHE1 or AE2-associated fluorescence staining in the negative control sections (data not shown) whereas with the GP sections, there was the suggestion of differential labeling for both transporters along the GP (Fig. 4). For NHE1, the fluorescent signal was distinct in the early PZ and was maintained through the late PZ and early HZ, before clearly decreasing in the middle to late HZ. For AE2, the fluorescence signal was low in the early PZ but clearly increased in the late PZ and

TABLE I. The Effect of DIDS and EIPA on Growth Plate Zone Height and Cell Density

Treatment (μM)	Total GP length (μm)	Late HZ length (μm)	HZ (% of total)	Late HZ cell density (cells/mm^2; n = 3)
Control (n = 4)	657 ± 99	144 ± 18	22.6 ± 1.8	4,383 ± 25
DIDS (250 μM; n = 6)	670 ± 76	116 ± 11	17.5 ± 0.7*	4,404 ± 884
Control (n = 5)	683 ± 99	147 ± 19	21.9 ± 1.1	4,007 ± 1,316
EIPA (444 μM; n = 5)	668 ± 68	117 ± 19	17.3 ± 1.5*	4,019 ± 1,300

Distal metatarsals from four to six P7 rats were cultured for 24 h in the absence/presence of DIDS or EIPA at the concentrations indicated. Bones were fixed, prepared, and visualized (see Materials and Methods Section). There was a significant reduction in height (%) of hypertrophic zone (HZ) from the total height of the growth plate in DIDS or EIPA-treated bones. However the average height of the growth plates and hypertrophic zone between control and treated bones were not significantly different. Hypertrophic zone cell density of treated bones also showed no significant difference from the control.
*Significantly different from the corresponding control ($P < 0.05$; unpaired Student's t-test; Data are means ± SEM for n experiments on separate animals).

remained elevated in the early HZ. To examine the overall semi-quantitative distribution pattern of NHE1 and AE2 in GPCs along P7 proximal tibia GP (S1–S8), the average fluorescence labeling intensity associated with membrane transporter localization was determined (see Materials and Methods Section). Figure 5 shows the relatively high level of NHE1 immunofluorescence throughout S1–S5 before decreasing from S6–S8 (one-way ANOVA; $P < 0.001$). The fluorescence intensity was significantly lower in S8 compared to the maximum intensity that was reached in S5 (Student's unpaired t-test; $P < 0.001$). For AE2, there was a significant increase in immunofluorescence intensity of AE2 throughout S1–S5 (one-way ANOVA; $P < 0.001$). The peak intensity was observed in S5, which was significantly higher than the original intensity recorded in S1 (unpaired Student's t-test; $P < 0.001$). After reaching the highest fluorescence intensity in S5, there was a significant decrease in the intensity from S6–S8 (one-way ANOVA; $P < 0.001$). The fluorescence intensity of AE2 in S8 was significantly lower than in S1 (Mann–Whitney test; $P = 0.008$). Although immunofluorescence labeling of both NHE1 and AE2 shared the highest intensity in S5 and the lowest in S8, the intensity of NHE1 in S1 was significantly higher than in AE2 (unpaired Student's t-test; $P < 0.005$). Figure 5 (inset) demonstrates a direct comparison between NHE1 and AE2 immunofluorescent intensity along GP with the data from the main figure being normalized to 100% at S5 (peak intensity in both graphs) to allow comparison. This indicates that while NHE1-immunofluorescent levels appeared higher throughout S1–S5, the AE2-immunofluorescence levels labeling was initially lower, but gradually increased towards S5. Both NHE1 and AE2-immunofluorescence labeling decreased dramatically after S5 toward S8.

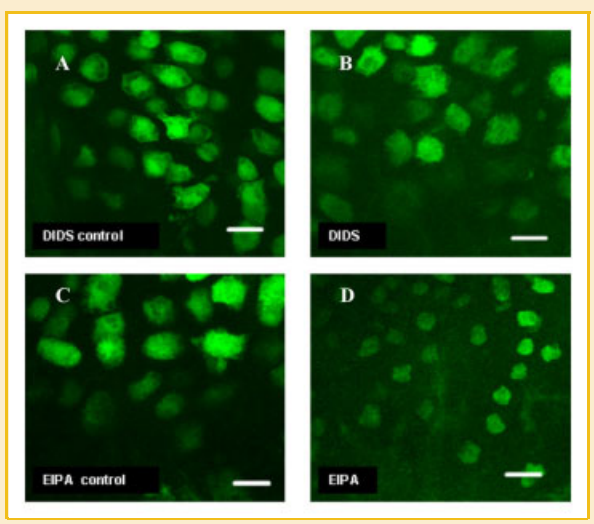

Fig. 3. The appearance of in situ HZ chondrocytes after culture with DIDS (250 μM) or EIPA (444 μM). Metatarsal bones were cultured in DIDS (A control, B) or EIPA (C control, D) for 24 h and labeled with CMFDA. Chondrocytes were then visualized by CLSM and regions of interest (ROIs) identified of in situ chondrocytes within the PZ and HZ (shown above), and images recorded for cell volume analysis (see Materials and Methods Section for details). Pooled data are presented in Table II. Scale bar = 20 μm in all panels. [Color figure can be seen in the online version of this article, available at http://wileyonlinelibrary.com/journal/jcb]

DISCUSSION

The rate of growth of P7 rat bone rudiments was markedly suppressed by EIPA and DIDS, both widely used inhibitors of the membrane transporters NHE1 and AE2 respectively in a range of cell types. The mechanism of inhibition, however, would appear to be different because although both drugs reduced the size of the HZ in relation to the overall length of the growth plate, EIPA significantly reduced the volume of chondrocytes throughout the length of the GP whereas DIDS had no significant effect (Table II). Fluorescence immunohistochemistry demonstrated that levels of NHE1 remained high in chondrocytes throughout most of the GP, but declined in late hypertrophic cells whereas AE2 levels demonstrated a biphasic effect (Fig. 5). Before proposing a role for these transporters in chondrocyte hypertrophy, it is important to consider potentially

TABLE II. The Effect of EIPA and DIDS on In Situ Growth Plate Chondrocyte Volume

	GPC volume (μm^3 from (n[N]))	
Treatment	PZC (S1–S2)	HZC (S7–S8)
Control	609 ± 46 (6[29])	1,880 ± 230 (6[44])
DIDS (250 μM)	572 ± 71 (3[25])	2,660 ± 419 (3[27])
Control	761 ± 50 (6[33])	2,044 ± 219 (6[38])
EIPA (444 μM)	211 ± 26* (3[15])	586 ± 54* (3[19])

Distal metatarsals from three to six P7 rats were cultured for 24 h in the absence/presence of DIDS or EIPA at the concentrations indicated. Bones were bisected, loaded with fluorescent dye (CMFDA), fixed and visualized using the CLSM technique (see Materials and Methods). Data are means ± SEM.
*Significant difference from the control ($P < 0.01$; unpaired Student's t-test).

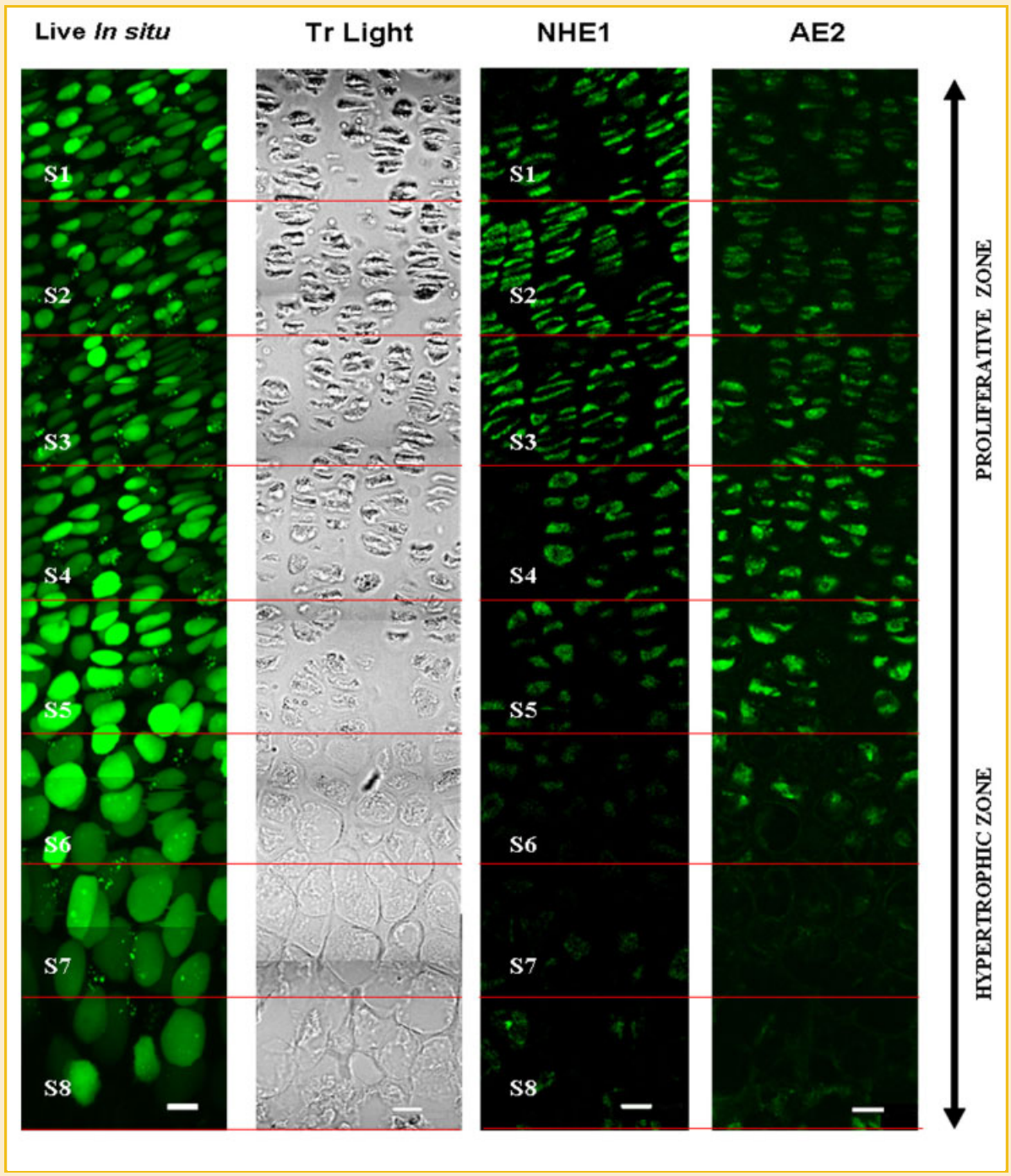

Fig. 4. Positive fluorescence signal associated with NHE1 and AE2 in the GP. Paraffin-embedded sections (10 μm) of proximal tibia from P7 rats showed positive fluorescence in GPC at different zone sections of proliferative zone and hypertrophic zone cells (S1–S8). Tr Light = transmitted light image corresponding to the fluorescence images. In situ GPC (figure far left) as viewed in unfixed live (calcein-loaded) GP tissue was shown for comparison. Images were taken using CLSM (63× objective). Bar = 20 μm. [Color figure can be seen in the online version of this article, available at http://wileyonlinelibrary.com/journal/jcb]

confounding effects which might complicate interpretation of the results.

The first issue is the specificity of the drugs used in this study. EIPA is a highly potent analogue of amiloride [Masereel et al., 2003] and a very effective inhibitor of NHEs in chondrocytes [Wilkins et al., 2000; Simpkin et al., 2007], with no reported inhibitory effects on other chondrocyte membrane transporters. However, DIDS is a relatively non-specific inhibitor of AEs [Cabantchik and Greger, 1992; Kidd and Thorn, 2000], as it also blocks Cl^- channels in a range of cell types [Okada, 1997] although at higher concentrations than those used here. DIDS does not however inhibit Cl^- channels in rabbit articular chondrocytes [Sugimoto et al., 1996]. DIDS at

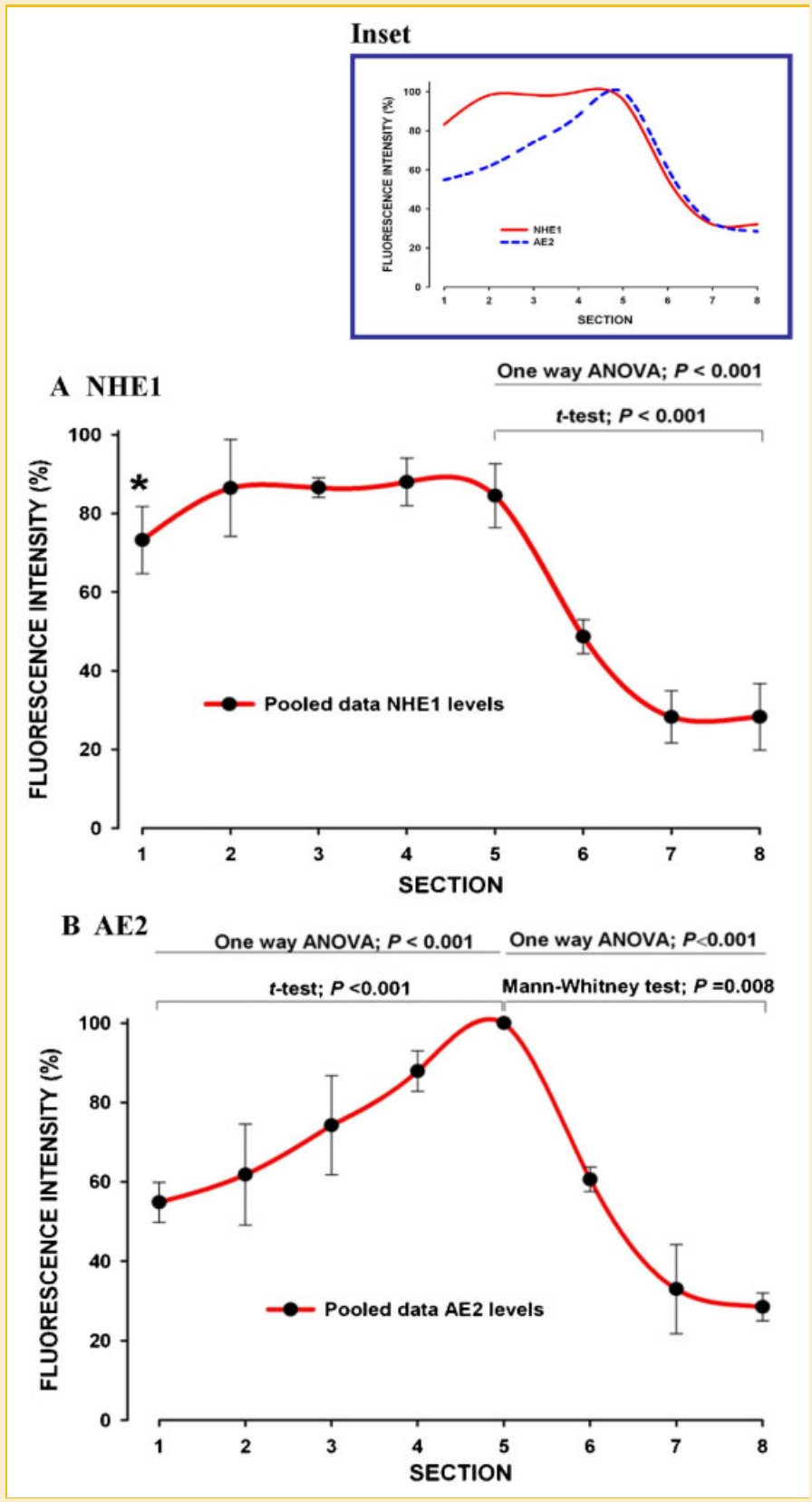

Fig. 5. Localization of NHE1 and AE2 in GPC along the GP. Chondrocyte-associated levels of (A) NHE1 and (B) AE2 fluorescence labeling are shown in the different sections along P7 rat proximal tibia GPs (see Materials and Methods Section for details). Data were pooled from five separate animals and at least 15 cells/section from each animal. Section 1 (S1) was nearest to the epiphyseal end and marked the early proliferative zone and section 8 (S8) was nearest to the metaphyseal end and denoted the late hypertrophic zone of the GP. The inset shows the graphs in (A) and (B) re-plotted together for comparison by normalizing the data to 100% at S5. *Significant difference compared to S1 of AE2 (unpaired Student's *t*-test; $P < 0.005$, $n = 5$). [Color figure can be seen in the online version of this article, available at http://wileyonlinelibrary.com/journal/jcb]

100 μM inhibits AE activity by >90% and bone growth by approximately 70% (Fig. 1A) but has only a minor effect (<10%) on volume-sensitive anion channels in cell types other than chondrocytes [Hallows et al., 1994] and therefore an inhibitory effect on GP chondrocyte Cl^- channels is unlikely to explain the inhibition of bone growth. DIDS has also been reported to block diastrophic dysplasia sulfate transport (DTDST)-mediated SO_4^- uptake which is essential for proteoglycan synthesis [Satoh et al., 1998]. However the concentration required (1 mM) is substantially higher than that required for inhibition of bone growth in the present study (Fig. 1A). Therefore EIPA would appear to give an accurate assessment of the role of NHEs in bone growth, and although DIDS is less specific, it is probable that the major effect of this drug on bone growth is mediated by inhibition of AE2s.

NHE1 is the principal isoform of this transporter in chondrocytes [Tattersall et al., 2003]. There is evidence that NHE3 is also present but normally dormant, however it can be stimulated by serum. We note that we did not include serum in our experiments and therefore it is unlikely that NHE3—if indeed present in growth plate chondrocytes—was unmasked. There is no strong evidence for NHE2 in chondrocytes [Tattersall et al., 2003]. Furthermore, careful studies by Gibson et al. [2009] showed that NHE activity of isolated chondrocytes was inhibited to the same extent by amiloride (1 mM) or the specific NHE1 inhibitor HOE694 (10 μM), supporting the notion that NHE1 is the principal isoform in chondrocytes. We therefore feel that it is unlikely that EIPA exerts unexpected effects on cells by acting on other NHE subtypes, and we are not aware of any inhibitory effects of EIPA on other chondrocyte membrane transporters other than NHE. Thus, NHE1 appears to be the principal isoform of this transporter in chondrocytes, and therefore it is unlikely that our results can be explained by unexpected effects of EIPA on other NHE subtypes.

It was necessary to raise the concentrations of drugs to relatively high levels in order to achieve the inhibitory effect on bone growth probably because of their relatively poor permeation through the connective tissue surrounding the bones to the GP chondrocytes. It should therefore be emphasized that the concentrations of drugs which finally reach the chondrocytes in situ within the growth plates, will be markedly less than the levels used in the culture medium (Fig. 1A,B). There was however concern that the drugs might simply be killing chondrocytes through a non-specific lethal action causing an apparent inhibition of bone growth. Nevertheless, we found that even after 24 h incubation with DIDS (250 μM) or EIPA (444 μM), there was no noticeable decrease in chondrocyte viability or density suggesting that such a non-specific toxic effect was unlikely and that a more subtle action involving inhibition of chondrocyte membrane transporters was probable.

Both inhibitors substantially (DIDS 87%; EIPA 81%; Fig. 1A,B) abolished bone growth, emphasizing an important role for membrane transporters in the control of bone lengthening. As both NHE1 and AE2 are involved in the control of pH_i and cell volume, it is difficult to disentangle the precise mechanism of action, however by also considering the FIHC data (Fig. 5) some pertinent observations can be made. For NHE1, cell-associated labeling was initially high until approximately S5 and then fell relatively rapidly in late hypertrophy in S6 and S7 with little further change in S8. The elevated levels of NHE1 prior to, and during hypertrophy might indicate the "housekeeping" role of this transporter to maintain optimal pH_i [Schelling and Abu Jawdeh, 2008] during cell enlargement and raised chondrocyte metabolism [Brighton et al., 1973; Hunziker et al., 1987]. The volume of in situ PZ and HZ chondrocytes in EIPA-treated rudiments was significantly (approx. threefold) less (Table II) than control cells in the same zones. However, the increase in volume of cells between these two zones was the same (approx. 2.7-fold) for both the control and EIPA-treated rudiments.

Cell volume is maintained relatively constant by the balance between membrane transporters which perform regulatory volume increase (RVI) and those that initiate regulatory volume decrease (RVD). At steady-state volume, these processes are balanced, however if transporters that are involved with either of these responses are inhibited, then there is likely to be a change in cell volume [O'Neill, 1999]. It is possible that this explains the reduced cell volume of chondrocytes in EIPA-treated rudiments (Table II) as this drug will suppress NHE1 potentially leading to cell shrinkage as the RVD transporters will continue to operate albeit at a low level. A reduction in hypertrophic chondrocyte volume is known to reduce the rate of longitudinal bone growth [Breur et al., 1991]. Thus it is possible that the inhibitory effect of EIPA on bone growth is due to a reduction in the set-point volume of chondrocytes and this could lead to delayed proliferation and/or differentiation of chondrocytes.

Although DIDS also inhibited the growth of bone rudiments, measurements of FIHC of AE2 along the GP suggested that the mechanism was different. Cell-associated levels of AE2 (Fig. 5B) demonstrated a biphasic trend and were initially significantly lower, but then increased to section S5 corresponding to early chondrocyte enlargement. Levels then decreased following the same trend as NHE1 labeling (Fig. 5 inset). The increased levels of AE2 with hypertrophy (Fig. 5B) strongly suggested that this transporter could be involved in the transition of chondrocytes from the PZ to the HZ and it is possible therefore that DIDS inhibits rudiment growth by suppressing this phase. There was no significant difference in the volume of chondrocytes within the PZC and the HZC in rudiments cultured in DIDS (Table II) suggesting that inhibition was not the result of preventing cell enlargement as suggested for the inhibitory effect of EIPA. It is possible that along with sustained levels of NHE1, the increased presence of AE2 during hypertrophy was required to maintain optimal pH_i in the face of the marked changes to chondrocyte metabolism occurring during hypertrophy. It was also noted that both EIPA and DIDS reduced the size of the HZ (compared to the length of the GP; Table I). This is known to be an important determinant of bone lengthening [Wilsman et al., 1996b] so although the sites of actions of the drugs and their effects on cell physiology might differ, the final common inhibitory effect is the same. It should also be remembered that fluorescent-labeling of the cytoplasmic space of chondrocytes using CMFDA or calcein is a convenient marker for cell viability, morphology and volume. However these dyes do not provide information about the physiological health of chondrocytes and it is likely that this will be adversely affected by the actions of DIDS or EIPA. Indeed it is probable that the inhibitory actions of these drugs on bone growth

will be mediated by changes to the physiological state of the cells although the precise mechanism(s) involved are currently unclear.

The decline in levels of both transporters with late hypertrophy is notable because it has been suggested that programmed cell death ("apoptosis") in some cell types is associated with a decline in AE2 levels [Hwang et al., 2009], and decreased levels of NHE1 are thought to facilitate apoptotic cell death by allowing intracellular acidification which is favorable for the activity of pro-apoptotic proteins [Schelling and Abu Jawdeh, 2008]. Many authors have described hypertrophic chondrocytes as dying by apoptosis [e.g., Adams and Shapiro, 2002]—the process of programmed cell death that plays an important role in physiological cell removal, in particular during foetal development [Wyllie et al., 1980]. However, the process by which hypertrophic chondrocytes die is morphologically distinct from apoptosis, for example, cell swelling and not shrinking precedes cell death, and hence Roach et al. [2004] proposed the term "chondroptosis" to describe the non-classical apoptosis of HZ chondrocytes, which results in ultimate self-destruction of the cell without the requirement of phagocytosis.

The present results implicate a role for NHE1 and AE2 in growth plate chondrocyte hypertrophy and it is important to recognize that a role of these transporters has already been established in studies on hypertrophy in other cell types. Increased protein and expression levels of NHE1 and its activation can promote hypertrophy for example in vascular smooth muscle cells [Hannan and Little, 1998], ventricular myocytes [Fliegel, 2009], and pulmonary artery smooth muscle cells [Yu and Hales, 2011]. On the other hand, pharmacological inhibition or silencing NHE1 by short interfering RNA (siRNA) inhibited proliferation and hypertrophy [Baartscheer et al., 2008; Yu and Hales, 2011]. There is however less information on the role of AE2 in cell proliferation and hypertrophy however the AE2(−/−) mouse suffers defective bone development/growth retardation and dies at or before weaning [Alper, 2006].

It seems intuitive that the expression, activity, and regulation of plasma membrane transporters must be involved in orchestrating the complex process of linear bone growth through supporting and driving the processes of chondrocyte proliferation, hypertrophy, and death—all of which are essential steps in bone lengthening [Bush et al., 2008a]. Although in avian growth plate there has been extensive research particularly regarding Ca^{2+} [Wuthier, 1993] and Na^+/P_i cotransport [e.g., Mansfield et al., 2001] mammalian growth plate chondrocytes have received relatively little attention. The inhibitory effects of EIPA and DIDS suggest that NHE1 and AE2 are closely involved in regulating bone growth (Fig. 1A,B). In addition, the finding that levels of these transporters change along the growth plate (Fig. 5) implies that they would be expected to be under the same hormonal control that regulates bone growth. It is possible therefore that membrane transporters could be a target for hormones (growth hormone, GH) and growth factors (e.g., IGF-1) that are already known to regulate growth rate and control chondrocyte hypertrophy and chondrocyte anabolism [Wang et al., 1999] but whose cellular sites of action are poorly understood. There is some evidence in support of this notion, for example in IGF-1 null mice where terminal hypertrophic chondrocytes are reduced in linear dimension and bone growth is suppressed, the expression of the insulin-sensitive glucose transporter GLUT4 is significantly reduced [Wang et al., 1999]. On the other hand, the addition of IGF-1 to isolated chondrocytes stimulates NHE1 [Tattersall and Wilkins, 2008] potentially resulting in an optimal pH_i for the early stages of chondrocyte hypertrophy. However it is clear that our knowledge of the various growth plate chondrocyte membrane transporters and the complex control of their expression and activity require detailed study if a full understanding of the lengthening of mammalian bone is possible.

ACKNOWLEDGMENTS

M.Y.L. was supported by Universiti Putra Malaysia (UPM) and the Ministry of Higher Education Malaysia under the Scheme of Academic Training for Bumiputera scholarships. C.F. is supported by an Institute Strategic Programme Grant from the Biotechnology and Biological Sciences Research Council (BBSRC). Funding was also provided by a BBSRC Project grant (BB/C513985/1) to ACH. We thank Dr. Michael Cousin for the donation of biological samples, Mr. P. McAuley for assistance with some experiments and Dr. T. Gillespie, Director of the IMPACT facility for assistance with CLSM.

REFERENCES

Adams CS, Shapiro IM. 2002. The fate of the terminally differentiated chondrocyte: Evidence for microenvironmental regulation of chondrocyte apoptosis. Crit Rev Oral Biol Med 13:465–473.

Alper S. 2006. Molecular physiology of SLC4 anion exchangers. Exp Physiol 91(1):153–161.

Amin AK, Huntley JS, Bush PG, Simpson AHRW, Hall AC. 2008. Osmolarity influences chondrocyte death in wounded articular cartilage. J Bone Joint Surg Am 90:1531–1542.

Baartscheer A, Hardziyenka M, Schumacher CA, Belterman CN, van Borren MM, Verkerk AO, Coronel R, Fiolet JW. 2008. Chronic inhibition of the Na^+/H^+—Exchanger causes regression of hypertrophy, heart failure, and ionic and electrophysiological remodelling. Br J Pharmacol 154(6):1266–1275.

Bancroft JD, Cook HC. 1994. Manual of histological techniques and their diagnostic application. Edinburgh: Churchill Livingstone.

Breur GJ, VanEnkevort BA, Farnum CE, Wilsman NJ. 1991. Linear relationship between the volume of hypertrophic chondrocytes and the rate of longitudinal bone growth in growth plates. J Orthop Res 9:348–359.

Brighton CT, Sugioka Y, Hunt RM. 1973. Cytoplasmic structures of epiphyseal plate chondrocytes. Quantitative evaluation using electron micrographs of rat costochondral junctions with special reference to the fate of hypertrophic cells. J Bone Joint Surg Am 55:771–784.

Buckwalter JA, Mower D, Ungar R, Schaeffer J, Ginsberg B. 1996. Morphometric analysis of chondrocyte hypertrophy. J Bone Joint Surg 68A: 243–255.

Bush PG, Hall AC. 2001a. Regulatory volume decrease (RVD) by isolated and *in situ* bovine articular chondrocytes. J Cell Physiol 187:304–314.

Bush PG, Hall AC. 2001b. The osmotic sensitivity of isolated and *in situ* bovine articular chondrocytes. J Orthop Res 19:768–778.

Bush PG, Wokosin DL, Hall AC. 2007. Two-versus one photon excitation laser scanning microscopy: Critical importance of excitation wavelength. Front Biosci 12:2646–2657.

Bush PG, Hall AC, Macnicol MF. 2008a. New insights into function of the growth plate: Clinical observations, chondrocyte enlargement and a possible role for membrane transporters. J Bone Joint Surg Br 90(12):1541–1547.

Bush PG, Parisinos CA, Hall AC. 2008b. The osmotic sensitivity of rat growth plate chondrocytes *in situ*; clarifying the mechanisms of hypertrophy. J Cell Physiol 214:621–629.

Bush PG, Pritchard M, Loqman MY, Damron TA, Hall AC. 2010. A key role for membrane transporter NKCC1 in mediating chondrocyte volume increase in the mammalian growth plate. J Bone Miner Res 25:1594–1603.

Cabantchik ZI, Greger R. 1992. Chemical probes for anion transporters of mammalian cell membranes. Am J Physiol 262:C803–C827.

Fliegel L. 2009. Regulation of the Na^+/H^+ exchanger in the healthy and diseased myocardium. Expert Opin Ther Targets 13(1):55–68.

Gibson JS, McCartney D, Sumpter J, Fairfax TPA, Milner PI, Edwards HL, Wilkins RJ. 2009. Rapid effects of hypoxia on H^+ homeostasis in articular chondrocytes. Pflugers Arch 458:1085–1092.

Hallows KR, Restrepo D, Knauf PA. 1994. Control of intracellular pH during regulatory volume decrease in HL-60 cells. Amer J Physiol 267:C1057–C1066.

Hannan KM, Little PJ. 1998. Mechanisms regulating the vascular smooth muscle Na/H exchanger (NHE-1) in diabetes. Biochem Cell Biol 76(5):751–759.

Hoffmann EK, Lambert IH, Pedersen SF. 2009. Physiology of cell volume regulation in vertebrates. Physiol Rev 89:193–277.

Hunziker EB. 1994. Mechanism of longitudinal bone growth and its regulation by growth plate chondrocytes. Microsc Res Tech 28:505–519.

Hunziker EB, Schenk RK, Cruz-Orive LM. 1987. Quantitation of chondrocyte performance in growth plate cartilage during longitudinal bone growth. J Bone Joint Surg Am 69:162–173.

Hwang J-M, Kao S-H, Hsieh Y-H, Li K-L, Wang P-H, Hsu L-S, Liu J-Y. 2009. Reduction of anion exchanger 2 expression induces apoptosis of human hepatocellular carcinoma cells. Mol Cell Biochem 327:135–144.

Kidd JF, Thorn P. 2000. Intracellular Ca^{2+} and Cl^- channel activation in secretory cells. Annu Rev Physiol 62:493–513.

Kiernan JA. 1999. Histological and histochemical methods: Theory and practice. Oxford: Butterworth-Heinemann.

Liu L, Schlesinger PH, Slack NM, Friedman PA, Blair HC. 2011. High capacity Na^+/H^+ exchange activity in mineralising osteoblasts. J Cell Physiol 226:1702–1712.

Loqman MY, Bush PG, Farquharson C, Hall AC. 2010. A cell shrinkage artefact in growth plate chondrocytes with common fixative solutions: Importance of fixative osmolarity for maintaining morphology. Eur Cells Mat 19:214–227.

Malo ME, Fliegel L. 2006. Physiological role and regulation of the Na^+/H^+ exchanger. J Physiol Pharmacol 84:1081–1095.

Mansfield K, Teixeira CC, Adams CS, Shapiro IM. 2001. Phosphate ions mediate chondrocyte apoptosis through a plasma membrane transporter mechanism. Bone 28:1–8.

Masereel B, Pochet L, Laeckmann D. 2003. An overview of inhibitors of Na^+/H^+ exchanger. Eur J Med Chem 38:547–554.

Okada Y. 1997. Volume expansion-sensing outward-rectifier Cl^- channel: Fresh start to the molecular identity and volume sensor. Am J Physiol 273: C755–C789.

O'Neill WC. 1999. Physiological significance of volume-regulatory transporters. Am J Physiol 276:C995–C1011.

Renshaw S. 2007. Immunochemical staining. In: Renshaw S, editor. Immunohistochemistry. Oxfordshire: Scion Publishing Limited. pp. 45–56.

Roach HI, Aigner T, Kouri JB. 2004. Chondroptosis: A variant of apoptotic cell death in chondrocytes? Apoptosis 9:265–277.

Satoh H, Susaki M, Shukunami C, Iyama K, Negoro T, Hiraki Y. 1998. Functional analysis of diastrophic dysplasia sulfate transporter. Its involvement in growth retardation of chondrocytes mediated by sulfated proteoglycans. J Biol Chem 273:12307–12315.

Schelling JR, Abu Jawdeh BG. 2008. Regulation of cell survival by Na^+/H^+ exchanger-1. Am J Physiol 295:F625–F632.

Shen M-R, Wilkins RJ, Chou C-Y, Ellory JC. 2002. Anion exchanger isoform 2 operates in parallel with Na^+/H^+ exchanger isoform 1 during regulatory volume decrease of human cervical cancer cells. FEBS Lett 512:52–58.

Simpkin VL, Murray DH, Hall AP, Hall AC. 2007. Bicarbonate-dependent pH_i regulation by chondrocytes within the superficial zone of bovine articular cartilage. J Cell Physiol 212:600–609.

Sugimoto T, Yoshino M, Nagao M, Ishii S, Yabu H. 1996. Voltage-gated ionic channels in cultured rabbit articular chondrocytes. Comp Biochem Physiol C Pharmacol Toxicol Endocrinol 115(3):223–232.

Tattersall AL, Wilkins RJ. 2008. Modulation of Na^+-H^+ exchange isoforms NHE1 and NHE3 by insulin-like growth factor-1 in isolated bovine articular chondrocytes. J Orthop Res 26:1428–1433.

Tattersall AL, Meredith D, Furla P, Shen MR, Ellory JC, Wilkins RJ. 2003. Molecular and functional identification of the $Na(^+)/H(^+)$ exchange isoforms NHE1 and NHE3 in isolated bovine articular chondrocytes. Cell Physiol Biochem 13(4):215–222.

Wang J, Zhou J, Bondy CA. 1999. Igf1 promotes longitudinal bone growth by insulin-like actions augmenting chondrocyte hypertrophy. FASEB J 13: 1985–1990.

Wilkins RJ, Browning JA, Ellory JC. 2000. Surviving in a matrix: Membrane transport in articular chondrocytes. J Memb Biol 177:95–108.

Wilsman NJ, Farnum CE, Green EM, Lieferman EM, Clayton MK. 1996a. Cell cycle analysis of proliferative zone chondrocytes in growth plates elongating at different rates. J Orthop Res 14:562–572.

Wilsman NJ, Farnum CE, Leiferman EM, Fry M, Barreto C. 1996b. Differential growth by growth plates as a function of multiple parameters of chondrocytic kinetics. J Orthop Res 14:927–936.

Wilsman NJ, Bernardini ES, Leiferman E, Noonan K, Farnum CE. 2008. Age and pattern of the onset of differential growth among growth plates in rats. J Orthop Res 26:1457–1465.

Wuthier RE. 1993. Involvement of cellular metabolism of calcium and phosphate in calcification of avian growth plate cartilage. J Nutr 123: 301–309.

Wyllie AH, Kerr JFR, Currie AR. 1980. Cell death: The significance of apoptosis. Int Rev Cytol 68:251–303.

Yu L, Hales CA. 2011. Silencing of sodium-hydrogen exchanger 1 attenuates the proliferation, hypertrophy, and migration of pulmonary artery smooth muscle cells via E2F1. Am J Respir Cell Mol Biol 45(5):923–930.